

Precursor of Superfluidity in a Strongly Interacting Fermi Gas with Negative Effective Range

Hiroyuki Tajima

*Theoretical Research Division, Nishina Center,
RIKEN, Wako, Saitama, 351-0198, Japan*

(Dated: March 15, 2022)

Abstract

We theoretically investigate the effects of pairing fluctuations in an ultracold Fermi gas near a Feshbach resonance with a negative effective range. By employing a many-body T -matrix theory with a coupled boson-fermion model, we show that the single-particle density of states exhibits the so-called pseudogap phenomenon which is a precursor of superfluidity induced by strong pairing fluctuations. We clarify the region where strong pairing fluctuations play a crucial role in single-particle properties, from the broad-resonance region to the narrow-resonance limit at the divergent two-body scattering length. We also extrapolate the effects of pairing fluctuations to the positive-effective-range region from our results near the narrow Feshbach resonance. Results shown in this paper are relevant to the connection between ultracold Fermi gases and low-density neutron matter from the viewpoint of finite-effective-range corrections.

PACS numbers: 03.75.Ss, 03.75.-b, 03.70.+k

I. INTRODUCTION

The realization of superfluidity in ultracold Fermi gases with pairing interactions, that are tunable by Feshbach resonances, is one of the most important breakthroughs in condensed matter physics [1–5]. The Bardeen-Cooper-Schrieffer-Bose-Einstein-condensation (BCS-BEC) crossover phenomenon [6–9] realized in ^6Li [1] and ^{40}K [2] Fermi gases has been extensively discussed in various fields such as FeSe superconductors [10–12], electron-hole systems [13, 14], nuclear matter [15–18], and color superconductivity in high-density quark matter [19–21].

In particular, the similarity between ultracold Fermi gases and dilute neutron matter in a neutron star has recently gathered much attention [22–25]. The idea is based on the fact that both systems are dominated by low-energy s -wave scatterings and the temperature T is very low compared to the Fermi temperature T_F . Since the neutron-neutron scattering length $a_{nn} = -18.5\text{fm}$ [26] is negatively large and the dimensionless interaction parameter is typically given by $1/k_F a_{nn} \simeq -0.03$ (where k_F is the Fermi momentum) at the nuclear saturation density $\rho_0 \simeq 0.17\text{fm}^{-3}$, the system property is very close to a unitary Fermi gas ($1/k_F a = 0$, where a is the two-body scattering length of Fermi atoms). In this regard, ground-state thermodynamic quantities have been experimentally measured with high precision [27, 28]. Moreover, the pairing gap [29–31], critical temperature [32–34], and thermodynamic quantities at finite temperature [34–36], which are important information for the cooling mechanism [37–42] as well as glitch phenomena [43–45] in a neutron star, have been also measured near the unitarity limit.

However, in addition to the scattering length, there is another key parameter, that is, the effective range r_e . While BCS-BEC crossover physics in ultracold Fermi gases are usually discussed with the zero-range contact-type interaction because the effective range is negligible near the broad Feshbach resonance, the effective range of neutron-neutron scatterings $r_{e,nn} = 2.8\text{fm}$ [26] is not negligible in the relevant density region of a neutron star. In this regard, effective-range corrections should be considered if one uses to treat an ultracold Fermi gas as a quantum simulator of neutron star matter. There are some theoretical studies on these corrections at $T = 0$ based on Quantum Monte-Carlo simulations [22, 23, 46] and the effective-range dependence of the ground-state energy has been reported. On the other hand, although its sign is generally different, finite *negative* effective range can be realized

in an ultracold Fermi gas with narrow Feshbach resonances [47]. We note that recently the optical control of scattering parameters with magnetic Feshbach resonance has also been proposed [48–50] and experimentally examined in a ^6Li Fermi gas [51, 52].

In this paper, we show how negative-effective-range corrections affect system properties in the presence of strong pairing fluctuations near the superfluid phase transition temperature T_c . It is well-known that a precursor of the superfluid phase transition can be seen in a strongly interacting Fermi gas through various physical quantities, (e. g., the enhancement of specific heat [34, 53] and suppression of spin susceptibility [54–62]). These strong-coupling effects are deeply related to the so-called pseudogap phenomenon [63–70], where the single-particle density of states near Fermi level shows a dip structure even above T_c . Although the pseudogap in an ultracold Fermi gas has not been directly observed in the experiment yet (indirectly observed in photo-emission spectra [71–73]), it exhibits when and how the Cooper pairing occurs from the microscopic viewpoint when the temperature approaches T_c in the normal phase. One can expect that such pairing properties have an important role in the cooling process of a neutron star across T_c . Actually, the pseudogap phenomenon has been also discussed in dilute nuclear matter [74–76].

We numerically calculate the single-particle density of states in a strongly interacting Fermi gas with negative effective range within the framework of the non-selfconsistent T -matrix approximation, which have been extensively used for the study of pseudogap physics in this system [64, 67, 68]. To reproduce the finite negative effective range associated with the narrow Feshbach resonance, we employ the so-called coupled fermion-boson model [77–80]. We obtain the pseudogap temperature T_{pg} , which is a characteristic temperature where pairing fluctuations are strongly enhanced, as a function of the negative effective range. As an application to neutron star physics, we also demonstrate how effects of pairing fluctuations in the small-positive-effective-range region can be extracted from results in the negative effective range region.

This paper is organized as follows. In Sec. II, we present the formalism of the non-selfconsistent T -matrix approximation with the coupled fermion-boson model. In Sec. III, we first review the BCS-BEC crossover physics with the negative effective range in this model. Subsequently, we present numerical results of the single-particle density of states in the BCS-BEC crossover regime. Throughout this paper, for simplicity, we set $\hbar = k_B = 1$ and the system volume is taken to be unity.

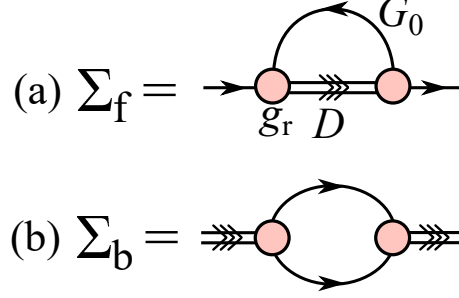


FIG. 1: The self-energy corrections of (a) Fermi atoms and (b) diatomic molecules. The single line (G_0) and double line (D) represent Green's functions of non-interacting atoms and dressed molecules, respectively. The shaded circle is the Feshbach coupling g_r .

II. FORMULATION

We start from the coupled fermion-boson model described by the Hamiltonian [77–80],

$$H = \sum_{\mathbf{p}, \sigma} \xi_{\mathbf{p}} c_{\mathbf{p}, \sigma}^\dagger c_{\mathbf{p}, \sigma} + \sum_{\mathbf{q}} (\varepsilon_{\mathbf{q}}/2 + 2\nu - 2\mu) b_{\mathbf{q}}^\dagger b_{\mathbf{q}} + g_r \sum_{\mathbf{p}, \mathbf{q}} (b_{\mathbf{q}}^\dagger c_{\mathbf{p}+\mathbf{q}/2, \uparrow} c_{-\mathbf{p}+\mathbf{q}/2, \downarrow} + \text{H.c.}). \quad (1)$$

Here, $c_{\mathbf{p}, \sigma}$ and $b_{\mathbf{q}}$ are the annihilation operators of a Fermi atom with the pseudospin $\sigma = \uparrow, \downarrow$ and a diatomic molecular boson, respectively. $\xi_{\mathbf{p}} = \varepsilon_{\mathbf{p}} - \mu$ is the kinetic energy of Fermi atoms measured from the chemical potential μ , where $\varepsilon_{\mathbf{p}} = p^2/2m$ (m is an atomic mass). The threshold energy of the diatomic molecule 2ν and the Feshbach coupling constant g_r are related to the two-body scattering length a and the effective range r_e , respectively. These relations are given by

$$\frac{4\pi a}{m} = -g_r^2 \left[2\nu - \sum_{\mathbf{p}} \frac{g_r^2}{2\varepsilon_{\mathbf{p}}} \right]^{-1} \equiv -\frac{g_r^2}{2\nu_r}, \quad (2)$$

$$r_e = -\frac{8\pi}{m^2 g_r^2}. \quad (3)$$

In Eq. (2), $2\nu_r$ is the renormalized threshold energy. For simplicity, we ignore the existence of non-resonant atom-atom scatterings.

We consider strong coupling effects in the framework of non-selfconsistent T -matrix approximation. The thermal Green's function of a Fermi atom G is given by

$$G(\mathbf{p}, i\omega_n) = \frac{1}{i\omega_n - \xi_{\mathbf{p}} - \Sigma_f(\mathbf{p}, i\omega_n)}, \quad (4)$$

where $\omega_n = (2n+1)\pi T$ is the fermion Matsubara frequency. Figure 1(a) shows the diagrammatic representation of the self-energy $\Sigma_f(\mathbf{p}, i\omega_n)$, which is in the form of,

$$\Sigma_f(\mathbf{p}, i\omega_n) = T \sum_{\mathbf{q}, \zeta_l} g_r^2 D(\mathbf{q}, i\zeta_l) G_0(\mathbf{q} - \mathbf{p}, i\zeta_l - i\omega_n), \quad (5)$$

where $G_0(\mathbf{p}, i\omega_n) = (i\omega_n - \xi_{\mathbf{p}})^{-1}$ is the bare Green's function of the Fermi atoms and $\zeta_l = 2l\pi T$ is the boson Matsubara frequency. The thermal Green's function of a dressed molecule $D(\mathbf{q}, i\zeta_l)$ includes the self-energy correction $\Sigma_b(\mathbf{q}, i\zeta_l)$ shown in Fig. 1(b) as follows:

$$D(\mathbf{q}, i\zeta_l) = \frac{1}{i\zeta_l - \varepsilon_{\mathbf{q}}/2 - 2\nu + 2\mu - \Sigma_b(\mathbf{q}, i\zeta_l)}. \quad (6)$$

$\Sigma_b(\mathbf{q}, i\zeta_l)$ is given by,

$$\Sigma_b(\mathbf{q}, i\zeta_l) = -g_r^2 \Pi(\mathbf{q}, i\zeta_l), \quad (7)$$

where,

$$\begin{aligned} \Pi(\mathbf{q}, i\zeta_l) &= T \sum_{\mathbf{p}, i\omega_n} G_0(\mathbf{p} + \mathbf{q}/2, i\omega_n + i\zeta_l) G_0(-\mathbf{p} + \mathbf{q}/2, -i\zeta_l) \\ &= - \sum_{\mathbf{p}} \frac{1 - f(\xi_{\mathbf{p}+\mathbf{q}/2}) - f(\xi_{-\mathbf{p}+\mathbf{q}/2})}{i\zeta_l - \xi_{\mathbf{p}+\mathbf{q}/2} - \xi_{-\mathbf{p}+\mathbf{q}/2}}, \end{aligned} \quad (8)$$

is the lowest-order particle-particle correlation function. In Eq. (8), $f(x) = 1/(e^{x/T} + 1)$ is the Fermi-Dirac distribution function. We note that the ultraviolet divergence of summation of \mathbf{p} in Eq. (8) can be avoided by the renormalization of ν . In this regard, Eq. (6) can be rewritten as

$$D(\mathbf{q}, i\zeta_l) = \frac{1}{i\zeta_l - \varepsilon_{\mathbf{q}}/2 - 2\nu_r + 2\mu + g_r^2 \left[\Pi(\mathbf{q}, i\zeta_l) - \sum_{\mathbf{p}} \frac{1}{2\varepsilon_{\mathbf{p}}} \right]}. \quad (9)$$

The superfluid phase transition temperature T_c is determined by the Hugenholtz-Pines condition [81] of Feshbach molecular bosons $[D(\mathbf{q} = 0, i\zeta_l = 0)]^{-1} = 0$, which reads,

$$\frac{m}{4\pi a} + \frac{2\mu}{g_r^2} + \sum_{\mathbf{p}} \left[\frac{1}{2\xi_{\mathbf{p}}} \tanh\left(\frac{\xi_{\mathbf{p}}}{2T_c}\right) - \frac{1}{2\varepsilon_{\mathbf{p}}} \right] = 0. \quad (10)$$

Eq. (10) is equivalent to the so-called Thouless criterion and recovers the ordinary gap equation of the single-channel model [64] at the broad-resonance limit ($g_r \rightarrow \infty$). We determine T_c and the critical chemical potential $\mu_c = \mu(T = T_c)$ by self-consistently solving Eq. (10) and particle number equation,

$$N = 2N_f + 2N_b$$

$$= 2T \sum_{\mathbf{p}, i\omega_n} G(\mathbf{p}, i\omega_n) + 2T \sum_{\mathbf{q}, i\zeta_l} D(\mathbf{q}, i\zeta_l), \quad (11)$$

where N is the total number. N_f and N_b are the numbers of Fermi atoms and Feshbach molecules, respectively.

In this paper, we calculate the single-particle density of states of a Fermi atom given by

$$\begin{aligned} \rho(\omega) &= \sum_{\mathbf{p}} A(\mathbf{p}, \omega) \\ &= -\frac{1}{\pi} \sum_{\mathbf{p}} \text{Im} G(\mathbf{p}, i\omega_n \rightarrow \omega + i\delta), \end{aligned} \quad (12)$$

where $A(\mathbf{p}, \omega)$ is the single-particle spectral function and ω is the single-particle energy. In Eq. (12), the analytic continuation ($i\omega_n \rightarrow \omega + i\delta$) is numerically done by using the Padé approximation with the small number $\delta = 10^{-2}\varepsilon_F$, where ε_F is the Fermi energy.

III. RESULTS

At first, we show the effective-range (Feshbach coupling) dependence of the superfluid phase transition temperature T_c and the critical chemical potential μ_c in the BCS-BEC crossover regime in Fig. 2. Here, $\tilde{g}_r = g_r\sqrt{N}/\varepsilon_F$ is the dimensionless Feshbach coupling, which is connected with the scaled effective range $r_e k_F = -32/(3\pi\tilde{g}_r^2)$. In the broad-resonance regime ($|r_e k_F| \lesssim 1$), T_c and μ_c are almost equal to the results of a previous work on the single-channel model [64]. In the strong-coupling BEC regime ($1/k_F a \gtrsim 1$), T_c and μ_c go to the BEC temperature of tightly bound molecular bosons $T_c^{\text{BEC}} = 0.218\varepsilon_F$ and the half of their binding energy $E_b/2 = -1/(2ma^2)$, respectively [8, 9, 64]. On the other hand, in the weak-coupling BCS regime ($1/k_F a \lesssim -1$), T_c approaches the famous BCS superfluid phase transition temperature $T_c^{\text{BCS}} \simeq 0.614T_F e^{-\frac{\pi}{2k_F a}}$ and μ_c becomes close to ε_F [7].

In the narrow-resonance regime, or large-negative-effective-range region ($|r_e k_F| \gtrsim 1$), T_c and μ_c deviate from results in the broad-resonance region. T_c increases with decreasing \tilde{g}_r where μ_c is positive ($1/k_F a \lesssim 0.31$). This enhancement of T_c is consistent with the previous work [82] which suggests that the narrow Feshbach resonance produces strong-pairing effects where the two-body bound state is absent. We note that T_c slightly decreases in the opposite side ($1/k_F a \gtrsim 0.31$). μ_c approaches 0 in the whole crossover region with decreasing g_r . In the large-negative-effective-range limit $r_e \rightarrow -\infty$ (narrow-resonance limit $g_r \rightarrow 0$), the system

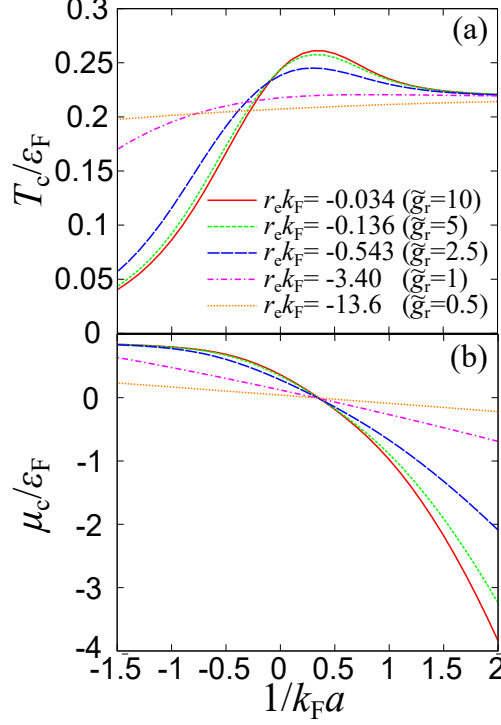


FIG. 2: (a) The superfluid phase transition temperature T_c and (b) the critical chemical potential μ_c in the whole BCS-BEC crossover regime with the finite effective range r_e . The quantity $\tilde{g}_r = g_r \sqrt{N}/\epsilon_F$ is the dimensionless Feshbach coupling.

can be exactly described by the mean-field theory since the self-energy corrections given by Eqs. (5) and (7) are proportional to g_r^2 . In this case, Eq. (11) becomes

$$\begin{aligned}
 N &= 2N_f^0 + 2N_b^0 \\
 &= 2 \sum_{\mathbf{p}} f(\xi_{\mathbf{p}}) + 2 \sum_{\mathbf{q}} b(\epsilon_{\mathbf{q}}/2 + 2\nu_r - 2\mu),
 \end{aligned} \tag{13}$$

where $b(x) = 1/(e^{x/T} - 1)$ is the Bose-Einstein distribution function. N_f^0 and N_b^0 in Eq. (13) represent the particle number of non-interacting Fermi atoms and diatomic molecules, respectively. One can evaluate μ_c from Eq. (13) with the condition of the gapless bosonic excitation as,

$$\mu_c = \nu_r = -\frac{mg_r^2}{8\pi a}, \tag{14}$$

which indicates $\mu_c = 0$ in this limit ($g_r \rightarrow 0$) with the finite scattering length. Substituting $\mu_c = 0$ to Eq. (13), one can obtain the critical temperature of the narrow resonance limit,

$$T_c^{\text{NRL}} = 0.204T_F. \tag{15}$$

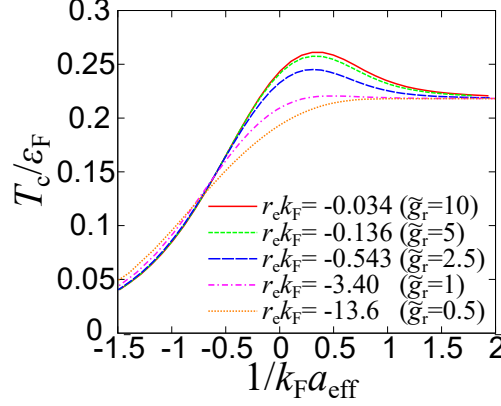


FIG. 3: The superfluid phase transition temperature T_c at various Feshbach couplings, as a function of $1/k_F a_{\text{eff}}$ where a_{eff} is the effective scattering length defined by Eq. (16).

Actually, T_c at $r_e k_F = -13.6$ ($\tilde{g}_r = 0.5$) shown in Fig. 2 (a) is very close to T_c^{NRL} .

In the narrow-resonance regime, it is known that an effective scattering length a_{eff} [80, 83] is useful to measure the interaction strength in the BCS-BEC crossover regime, defined by

$$\frac{4\pi a_{\text{eff}}}{m} = -\frac{g_r^2}{2\nu_r - 2\mu}, \quad (16)$$

since the effective-interaction strength between Fermi atoms is given by $U_{\text{eff}}(\mathbf{q}, i\zeta_l) = -g_r^2 D(\mathbf{q}, i\zeta_l)$. Indeed, using a_{eff} , one can find that Eq. (10) can be rewritten as

$$\frac{m}{4\pi a_{\text{eff}}} + \sum_{\mathbf{p}} \left[\frac{1}{2\xi_{\mathbf{p}}} \tanh\left(\frac{\xi_{\mathbf{p}}}{2T_c}\right) - \frac{1}{2\varepsilon_{\mathbf{p}}} \right] = 0. \quad (17)$$

Eq. (17) is the same form of the ordinary BCS gap equation in the single-channel model [64]. Fig. 3 shows T_c as a function of $1/k_F a_{\text{eff}}$ at various Feshbach couplings. Although T_c quantitatively changes if one tunes g_r in the intermediate region ($-1 \lesssim 1/k_F a_{\text{eff}} \lesssim 1$), both weak-coupling and strong-coupling regimes except the above region do not depend on g_r . In this regard, in the case of narrow resonance, it is appropriate that the weak-coupling BCS regime and the strong-coupling BEC regime are defined as $1/k_F a_{\text{eff}} \lesssim -1$ and $1/k_F a_{\text{eff}} \gtrsim 1$, respectively.

Fig. 4 shows the effective-range dependence of $1/k_F a_{\text{eff}}$ in the crossover region ($1/k_F a_{\text{eff}} = -0.5, 0$, and 0.5) at $T = T_c$. We also show the Feshbach coupling dependence of $1/k_F a_{\text{eff}}$ in the inset of Fig. 4. In the narrow-resonance limit, one can find that $1/k_F a_{\text{eff}} \simeq 0.31$ (where $\mu_c = 0$) at each scattering length. This is nothing but the reason why the narrow

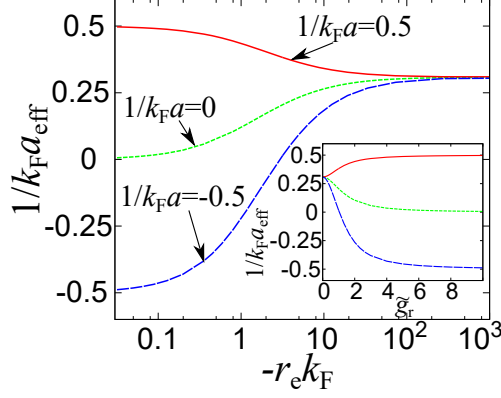


FIG. 4: The effective range dependence of the inverse effective scattering length $1/k_F a_{\text{eff}}$ at $1/k_F a = -0.5$ (solid line), 0 (dotted line) and 0.5 (dashed line) at $T = T_c$. The inset shows $1/k_F a_{\text{eff}}$ as a function of the dimensionless Feshbach coupling \tilde{g}_r . In each figure, we use the same line style at each scattering length.

Feshbach resonance induces a strong attraction between Fermi atoms and T_c is enhanced by the negative effective range in the region where $1/k_F a \lesssim 0$ shown in Fig. 2 (a).

In Fig. 5, we show the Feshbach coupling dependence of particle numbers in the crossover region. The particle number of Fermi atoms $2N_f$ are divided into two parts,

$$\begin{aligned} 2N_f &= 2N_f^0 + 2\delta N_f \\ &= 2 \sum_{\mathbf{p}} f(\xi_{\mathbf{p}}) + 2T \sum_{\mathbf{p}, i\omega_n} [G(\mathbf{p}, i\omega_n) - G_0(\mathbf{p}, i\omega_n)], \end{aligned} \quad (18)$$

where the second term $2\delta N_f$ is the fluctuation corrections. δN_f monotonically increases with increasing the interaction strength from $1/k_F a = -0.5$ [Fig. 5(a)] to 0.5 [Fig. 5(c)]. On the other hand, $2\delta N_f$ monotonically decreases with decreasing g_r at each scattering length and the total Fermi atomic number becomes dominated by the non-interacting part $2N_f^0$. In the narrow resonance limit, $2N_f^0$ at $T = T_c^{\text{NRL}}$ ($\mu_c = 0$) approaches a constant value given by

$$\begin{aligned} 2N_f &\simeq 2N_f^0 = 2 \sum_{\mathbf{p}} f(\varepsilon_{\mathbf{p}}) \\ &\simeq 0.0937N. \end{aligned} \quad (19)$$

In contrast to $2N_f$, the particle number of diatomic molecular bosons $2N_b$ increases with decreasing g_r and finally reaches $N - 2N_f^0 \simeq 0.906N$ in the narrow resonance limit. This interplay of $2N_f$ and $2N_b$ and the suppression of the fluctuation contribution $2\delta N_f$ in spite

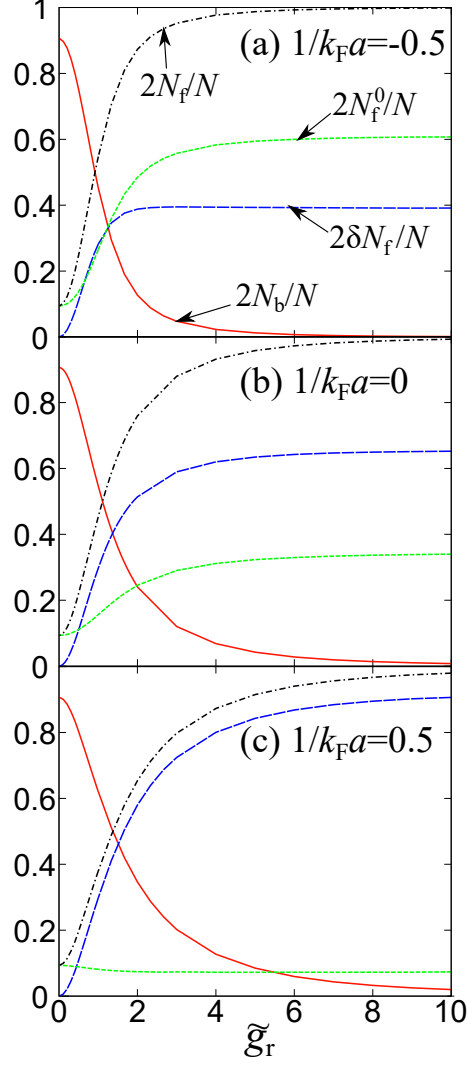


FIG. 5: Particle numbers as a function of dimensionless Feshbach coupling \tilde{g} at $1/k_F a = -0.5$ (a), 0 (b), and 0.5 (c) at $T = T_c$.

of the strong attraction between atoms are characteristic features of narrow Feshbach resonances that can not be seen in broad Feshbach resonances.

Fig. 6 shows the single-particle density of states $\rho(\omega)$ in the crossover regime at $T = T_c$ with negative effective range, where $\rho_0(\omega = 0) = mk_F/(2\pi^2)$ is the single-particle density of states at the Fermi level in a non-interacting Fermi gas at $T = 0$. In the weak-coupling side $1/k_F a = -0.5$ (a), one can see that the pseudogap phenomenon appears as a dip structure around $\omega = 0$ at the broad resonance ($r_e k_F = -0.034$). This pseudogap size is enhanced with decreasing g_r in the broad resonance region ($\tilde{g}_r \gtrsim 1$). However, the pseudogap closes

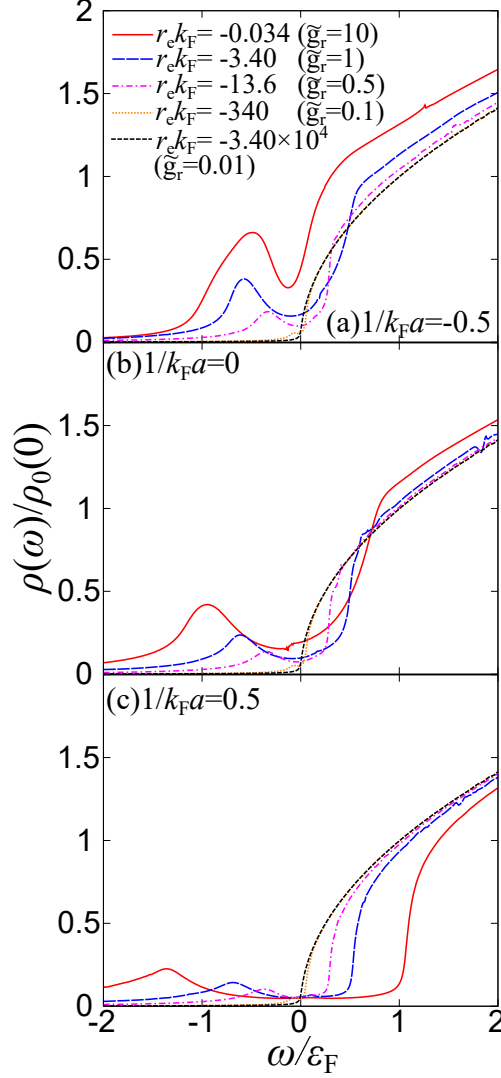


FIG. 6: Single-particle density of states $\rho(\omega)$ at $T = T_c$ with various effective ranges [$1/k_F a = -0.5$ (a), 0 (b), 0.5 (c)]. $\rho_0(0)$ is the single-particle density of states at the Fermi level in an ideal Fermi gas at $T = 0$.

with decreasing g_r in the narrow resonance region ($\tilde{g}_r \lesssim 1$). This fact can be understood by considering the static approximation [64, 84] given by

$$\Sigma_f(\mathbf{p}, i\omega_n) \simeq -\Delta_{\text{pg}}^2 G_0(-\mathbf{p}, -i\omega_n), \quad (20)$$

where,

$$\begin{aligned} \Delta_{\text{pg}}^2 &= -T \sum_{\mathbf{q}, i\zeta_l} g_r^2 D(\mathbf{q}, i\zeta_l) \\ &= g_r^2 N_b, \end{aligned} \quad (21)$$

is the so-called pseudogap parameter which is directly related to g_r as well as N_b . We note that this approximation is justified near T_c where $D(\mathbf{q} = 0, i\zeta_l = 0)$ diverges. By substituting Eq. (20) to Eq. (4), one can obtain,

$$G(\mathbf{p}, i\omega_n) \simeq \frac{i\omega_n + \xi_p}{(i\omega_n)^2 - \xi_p^2 - \Delta_{pg}^2}. \quad (22)$$

Eq. (22) shows that $G(\mathbf{p}, i\omega_n)$ becomes similar to the BCS Green's function even above T_c due to strong pairing fluctuations. In this regard, the pseudogap size is determined by Δ_{pg} where $\mu > 0$. Since N_b monotonically increases with decreasing g_r as shown in Fig. 5, Δ_{pg} also increases in the broad-resonance region. However, in the narrow-resonance region, Δ_{pg} is proportional to g_r and disappear at $g_r \rightarrow 0$ because N_b becomes almost constant. On the other hand, in the strong-coupling side $1/k_F a = 0.5$ (c) where $\mu_c < 0$, the gap size in $\rho(\omega)$ is given by $2\sqrt{\mu_c^2 + \Delta_{pg}^2}$. This value depends on μ_c rather than Δ_{pg} . In the strong-coupling limit with the broad resonance, this energy gap is given by the binding energy of bound molecules where $2|\mu_c| \simeq E_b = 1/ma^2$ [7, 64]. In the narrow-resonance regime where $\mu_c < 0$, the energy gap monotonically disappears since both μ_c and Δ_{pg} approach 0 with decreasing g_r .

We note that in the case of the broad-resonance limit ($r_e \rightarrow 0$), Δ_{pg} is related to Tan's contact C [85–87], which can be represented by $C = m^2 \Delta_{pg}^2$ [89]. In the coupled fermion-boson model, it is given by [88],

$$C = m^2 g_r^2 N_b = -\frac{8\pi N_b}{r_e}. \quad (23)$$

Although Tan's relation is developed in the case of the zero-range contact potential, how the finite effective range affects C in the whole BCS-BEC crossover region is an interesting problem left as a future work.

Figure 7 shows the temperature dependence of $\rho(\omega)$ at $1/k_F a = 0$, where $r_e k_F = -0.034$ (a), -3.40 (b) and -16.3 (c). The pseudogap is gradually smeared due to thermal fluctuations with increasing T and the dip structure disappears at high temperature. In the high temperature region ($T \gtrsim 0.5T_F$), $\rho(\omega)$ qualitatively corresponds to the density of states in a non-interacting Fermi gas given by $\rho_0(\omega) = \frac{m}{2\pi^2} \sqrt{2m(\omega + \mu)}$. In the narrow-resonance region [$r_e k_F = -16.3$ as shown in Fig. 7 (c)], the pseudogap structure disappears at lower temperature than in the case of the broad Feshbach resonance since the pseudogap size is also smaller at $T = T_c$. In this paper, we introduce the pseudogap temperature T_{pg} [64]

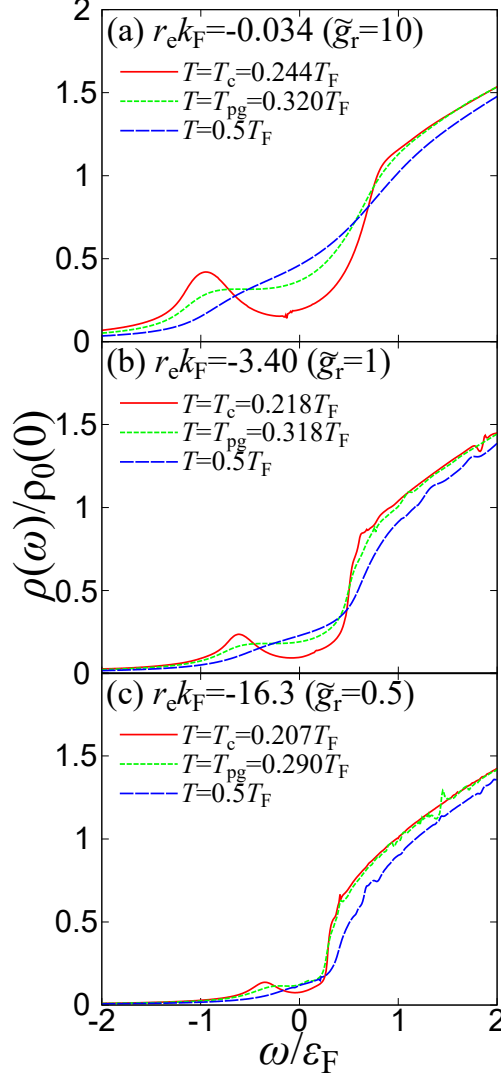


FIG. 7: The single-particle density of states $\rho(\omega)$ at $1/k_F a = 0$ at the different temperatures. In each figure, the solid, dotted, and dashed lines represent results of $T = T_c$, T_{pg} , and $0.5T_F$, respectively. Here T_{pg} is the pseudogap temperature defined as the temperature where the dip structure in $\rho(\omega)$ disappears. We set the effective range $r_e k_F = -0.034$ (a), -3.40 (b), and -16.3 (c).

which is a characteristic temperature where the dip structure in $\rho(\omega \simeq 0)$ disappears, shown as the dotted lines in Fig. 7. Although the definition of this characteristic temperature has some ambiguity because the pseudogap is a crossover phenomenon without any distinct changes of properties like a phase transition, one can expect that the system properties are dominated by strong pairing fluctuations which cannot be explained by the mean-field the-

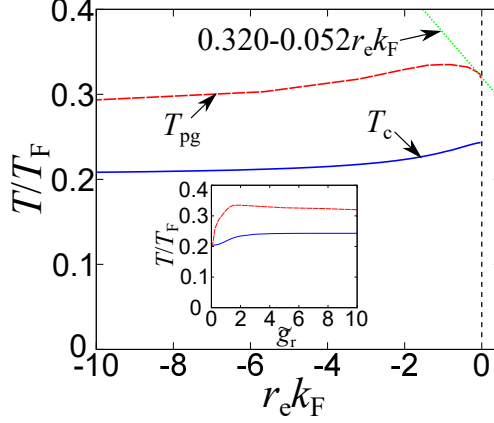


FIG. 8: The superfluid phase transition temperature T_c (solid line) and the pseudogap temperature T_{pg} (dashed line) as a function of the effective range r_e at $1/k_F a = 0$. The dotted line shows the linear fitting of T_{pg} in the small negative effective range region ($|r_e k_F| \lesssim 0.05$). The inset shows T_c and T_{pg} versus the dimensionless Feshbach coupling \tilde{g}_r .

ory or the Fermi-liquid theory below T_{pg} . Actually, a similar characteristic temperature can be observed via the temperature dependence of thermodynamic quantities such as specific heat [53] and spin susceptibility [59].

Fig. 8 shows the negative-effective-range dependence of T_c and T_{pg} at $1/k_F a = 0$. In the broad-resonance region ($r_e k_F \gtrsim -1$), T_{pg} is slightly enhanced with decreasing r_e reflecting the increase of Δ_{pg} . In the narrow resonance regime ($r_e k_F \lesssim -1$), T_{pg} gradually decreases with decreasing r_e and as shown in the inset of Fig. 8, T_{pg} coincides with T_c around $\tilde{g}_r \simeq 0.08$, where the corresponding effective range is given by $r_e k_F \simeq -5.3 \times 10^2$. Beyond this value, the system properties can be described by the mean-field theory even near T_c .

Using results shown in Fig. 8, we demonstrate applications to dilute neutron matter which has a positive effective range in the neutron-neutron scattering. At $1/k_F a = 0$, it is known that the ground-state energy $E(r_e k_F)$ with a small effective range can be expressed as [46, 90],

$$\frac{E(r_e k_F)}{E_{FG}} = \xi_B + \zeta r_e k_F + O(r_e^2 k_F^2), \quad (24)$$

where $E_{FG} = \frac{3}{5} N \epsilon_F$ is the ground-state energy of an ideal Fermi gas. In Eq. (24), ξ_B and ζ are the Bertsch parameter [91] and the linear coefficient with respect to $r_e k_F$, respectively. Recently, ξ_B and ζ have been determined by QMC simulations [23, 46, 90]. Moreover, ξ_B

has been precisely measured in current experiments [27, 34, 92]. Analogously, we expand T_{pg} with respect to $r_e k_F$ and determine the linear coefficient from the fitting of T_{pg} in the small-negative-effective-range region ($|r_e k_F| \lesssim 0.05$). As a result, we obtain

$$\frac{T_{\text{pg}}(r_e k_F)}{T_F} = 0.320 - 0.052 r_e k_F + O(r_e^2 k_F^2). \quad (25)$$

In the small effective range region, one can expect that Eq. (25) is valid even for the *positive* effective range. In this sense, from Eq. (25), one can find that pairing fluctuations seem to be suppressed by the positive effective range since T_{pg} decreases with increasing $r_e (> 0)$. This estimation is expected to be reasonable since the positive effective range suppresses the magnitude of the scattering phase shift which characterizes the interaction strength. It can be an important information for astrophysical simulations or studies on the cooling process of a neutron star [41]. We emphasize that this characteristic temperature originating from strong pairing fluctuations can be determined in cold-atom experiments through the measurement of thermodynamic quantities such as spin susceptibility, which is now experimentally accessible [93–95].

We note that the same analysis can be applied to T_c but it is necessary to consider effects of particle-hole fluctuations [96–98] to obtain the correct effective-range dependence of T_c . Indeed, the non-selfconsistent T -matrix approximation overestimates $T_c \simeq 0.24 T_F$ in the unitarity limit ($1/k_F a = 0$, $r_e = 0$) compared to the experimental value $0.167(13) T_F$ [34]. Although the particle-hole fluctuations may affect T_{pg} , we expect that our result for T_{pg} is qualitatively unchanged since the non-selfconsistent T -matrix approximation can successfully explain effects of pairing fluctuations on the recent experimental results of local photoemission spectra in the pseudogap regime [99].

IV. SUMMARY

To summarize, we have theoretically investigated the effects of pairing fluctuations in a strongly interacting Fermi gas with negative effective range. Within the framework of the non-selfconsistent T -matrix approximation with the coupled fermion-boson model for the narrow Feshbach resonance, we have discussed the negative-effective-range corrections on the single-particle density of states at the superfluid phase transition temperature T_c in the BCS-BEC crossover regime.

On the weak coupling side $1/k_F a \lesssim 0$ where the critical chemical potential is positive ($\mu_c > 0$), the negative-effective-range corrections induce strong pairing effects and the pseudogap size at T_c is enhanced in the broad-resonance regime ($|r_e k_F| \lesssim 1$). On the other hand, on the strong coupling side $1/k_F a \gtrsim 0$ where $\mu_c < 0$, the effective interaction strength is weakened due to the presence of the negative effective range and the pseudogap size monotonically decreases with decreasing r_e . Approaching the narrow-resonance limit ($r_e \rightarrow -\infty$, $g_r \rightarrow 0$), the system's properties are exactly described by the mean field theory and the pseudogap disappears at each scattering length.

At $1/k_F a = 0$, we have shown the negative-effective-range dependence of the pseudogap temperature T_{pg} , which is one of the characteristic temperatures where strong pairing fluctuations affect physical quantities. While in the broad-resonance region ($|r_e k_F| \lesssim 1$), T_{pg} increases with decreasing r_{pg} , the pseudogap region ($T_c < T < T_{pg}$) disappears in the deep-narrow-resonance regime ($r_e k_F \lesssim -5.3 \times 10^2$).

From the negative-effective-range dependence of T_{pg} in the broad-resonance region, we have obtained $T_{pg}/T_F = 0.320 - 0.052 r_e k_F + O(r_e^2 k_F^2)$. This equation is expected to be valid even in the small-*positive*-effective-range region, indicating that pairing fluctuations is suppressed by the small positive effective range. Since the effects of strong pairing fluctuations near T_c in interacting fermions is quite non-trivial and crucial for an ultracold Fermi gas as well as neutron star physics, our strategy suggests that the experimental realization of a strongly interacting Fermi gas with negative effective range can contribute toward the further understanding of such interdisciplinary topics.

The negative-effective-range dependence of other physical observables remains as an interesting topic for future work. The diagrammatic approach presented in this paper can be extended to study thermodynamic quantities such as spin susceptibility. It would also be interesting to study how the negative-effective-range region connects to the positive side in the BCS-BEC crossover regime, as well as the extension to the superfluid phase.

Acknowledgments

The author thanks P. Naidon for kindly reading the manuscript and suggesting improvements, and T. Hatsuda, Y. Ohashi, S. Uchino, Y. Nishida, and D. Kagamihara for useful

discussions. This work was supported by a Grant-in-Aid for JSPS fellows (No.17J03975).

- [1] C. A. Regal, M. Greiner, and D. S. Jin, Phys. Rev. Lett. **92**, 040403 (2004).
- [2] M. W. Zwierlein, C. A. Stan, C. H. Schunck, S. M. F. Raupach, A. J. Kerman, and W. Ketterle, Phys. Rev. Lett. **92**, 120403 (2004).
- [3] S. Giorgini, S. Pitaevskii, and S. Stringari, Rev. Mod. Phys. **80**, 1215 (2008).
- [4] I. Bloch, J. Dalibard, and W. Zwerger, Rev. Mod. Phys. **80**, 885 (2008).
- [5] C. Chin, R. Grimm, P. Julienne, and E. Tiesinga, Rev. Mod. Phys. **82**, 1225 (2010).
- [6] D. M. Eagles Phys. Rev. **186**, 456 (1969).
- [7] A. J. Leggett, in *Modern Trends in the Theory of Condensed Matter*, edited by A. Pekalski and J. Przystawa (Springer Verlag, Berlin, 1980), p. 14.
- [8] P. Nozières and S. Schmitt-Rink, J. Low Temp. Phys. **59**, 195 (1985).
- [9] C. A. R. Sa de Melo, M. Randeria, and J. R. Engelbrecht, , Phys. Rev. Lett. **71**, 3202 (1993).
- [10] S. Kasahara, T. Watashige, T. Hanaguri, Y. Kohsaka, T. Yamashita, Y. Shimoyama, Y. Mizukami, R. Endo, H. Ikeda, Proc. Natl. Acad. Sci. U.S.A. **111**, 16309 (2014).
- [11] S. Kasahara, T. Yamashita, A. Shi, R. Kobayashi, Y. Shimoyama, T. Watashige, K. Ishida, T. Terashima, T. Wolf, F. Hardy et al., Nat. Commun. **7**, 12843 (2016)
- [12] H. Yang, G. Chen, X. Zhu, J. Xing, and H.-H. Wen, Phys. Rev. B **96**, 064501 (2017).
- [13] Y. Tomio, K. Honda, and T. Ogawa, Phys. Rev. B **73**, 235108 (2006).
- [14] B. Zenker, D. Ihle, F. X. Bronold, and H. Fehske, Phys. Rev. B **85**, 121102(R) (2012).
- [15] U. Lombardo, P. Nozières, P. Schuck, H.-J. Schulze, and A. Sedrakian, Phys. Rev. C **64**, 064314 (2001).
- [16] M. Matsuo, Phys. Rev. C **73**, 044309 (2006).
- [17] J. Margueron, H. Sagawa, and K. Hagino, Phys. Rev. C **76**, 064316 (2007).
- [18] M. Jin, M. Urban, and P. Schuck, Phys. Rev. C **82**, 024911 (2010).
- [19] Y. Nishida and H. Abuki, Phys. Rev. D **72**, 096004 (2005).
- [20] H. Abuki, Nucl. Phys. A **791**, 117 (2007).
- [21] H. Abuki, G. Baym, T. Hatsuda, and N. Yamamoto, Phys. Rev. D **81**, 125010 (2010).
- [22] A. Gezerlis and J. Carlson, Phys. Rev. C **77**, 032801(R) (2008).
- [23] M. M. Forbes, S. Gandolfi, and A. Gezerlis, Phys. Rev. A **86**, 053603 (2012).

- [24] P. van Wyk, H. Tajima, D. Inotani, A. Ohnishi, and Y. Ohashi, *Phys. Rev. A* **97**, 013601 (2018).
- [25] A. Schwenk and C. J. Pethick, *Phys. Rev. Lett.* **95**, 160401 (2005).
- [26] R. B. Wiringa, V. G. J. Stoks, and R. Schiavilla, *Phys. Rev. C* **51**, 38 (1995).
- [27] M. Horikoshi, M. Koashi, H. Tajima, Y. Ohashi, and M. Kuwata-Gonokami, *Phys. Rev. X* **7**, 041004 (2017).
- [28] H. Tajima, P. van Wyk, R. Hanai, D. Kagamihara, D. Inotani, M. Horikoshi, and Y. Ohashi, *Phys. Rev. A* **95**, 043625 (2017).
- [29] C. Chin, M. Bartenstein, A. Altmeyer, S. Riedl, S. Jochim, J. H. Denschlag, and R. Grimm, *Science* **305**, 1128 (2004).
- [30] A. Schirotzek, Y. I. Shin, C. H. Schunck, and W. Ketterle, *Phys. Rev. Lett.* **101**, 140403 (2008).
- [31] S. Hoinka, P. Dyke, M. G. Lingham, J. J. Kinnunen, G. M. Bruun, and C. Vale, *Nat. Phys.* **13**, 943 (2017).
- [32] L. Luo, B. Clancy, J. Joseph, J. Kinast, and J. E. Thomas, *Phys. Rev. Lett.* **98**, 080402 (2007).
- [33] Y. Inada, M. Horikoshi, S. Nakajima, M. Kuwata-Gonokami, M. Ueda, and T. Mukaiyama, *Phys. Rev. Lett.* **101**, 180406 (2008).
- [34] M. J. H. Ku, A. T. Sommer, L. W. Cheuk, and M. W. Zwierlein, *Science* **335**, 563 (2012).
- [35] M. Horikoshi, S. Nakajima, M. Ueda, and T. Mukaiyama, *Science* **327**, 442 (2010).
- [36] S. Nascimbène, N. Navon, K. J. Jiang, F. Chevy and C. Salomon, *Nature* **463**, 1057 (2010).
- [37] E. Flowers, M. Ruderman, and P. Sutherland, *Astrophys. J.*, **205**, 541 (1976).
- [38] D. Page, J. M. Lattimer, M. Prakash, and A. W. Steiner, *Astrophys. J.*, **707**, 1131 (2009).
- [39] P. S. Shternin, D. G. Yakovlev, C. O. Heinke, W. C. G. Ho, D. J. Patnaude, *Mon. Not. Roy. Astron. Soc.* **412**, L108 (2011).
- [40] D. Page, M. Prakash, J. M. Lattimer, and A. W. Steiner, *Phys. Rev. Lett.* **106**, 081101 (2011).
- [41] M. Oertel, M. Hempel, T. Klähn, and S. Typel, *Rev. Mod. Phys.* **89**, 015007 (2017).
- [42] A. Sedrakian and J. W. Clark, *arXiv1802.00017 [nucl-th]*.
- [43] P. W. Anderson and N. Itoh, *Nature* **256**, 25 (1975).
- [44] T. Delsate, N. Chamel, N. Gürlebeck, A. F. Fantina, J. M. Pearson, and C. Ducoin, *Phys. Rev. D* **94**, 023008 (2016).
- [45] W. C. G. Ho, C. M. Espinoza, D. Antonopoulou, and N. Andersson, *JPS Conf. Proc.* **14**,

- 010805 (2017).
- [46] L. M. Schonenberg and G. J. Conduit, Phys. Rev. A **95**, 013633 (2017).
 - [47] E. L. Hazlett, Y. Zhang, R. W. Stites, and K. M. O'Hara, Phys. Rev. Lett. **108**, 045304 (2012).
 - [48] D. M. Bauer, M. Lettner, C. Vo, G. Rempe, and S. Dürr, Nat. Phys. **5**, 339 (2009).
 - [49] H. Wu and J. E. Thomas, Phys. Rev. Lett. **108**, 010401 (2012).
 - [50] H. Wu and J. E. Thomas, Phys. Rev. A **86**, 063625 (2012).
 - [51] M. Semczuk, W. Gunton, W. Bowden, and K. W. Madison, Phys. Rev. Lett. **113**, 055302 (2014).
 - [52] A. Jagannathan, N. Arunkumar, J. A. Joseph, and J. E. Thomas, Phys. Rev. Lett. **116**, 075301 (2016).
 - [53] P. van Wyk, H. Tajima, R. Hanai, and Y. Ohashi, Phys. Rev. A **93**, 013621 (2016).
 - [54] T. Kashimura, R. Watanabe, and Y. Ohashi, Phys. Rev. A **86**, 043622 (2012).
 - [55] F. Palestini, P. Pieri, and G. C. Strinati, Phys. Rev. Lett. **108**, 080401 (2012).
 - [56] M. P. Mink, V. P. J. Jacobs, H. T. C. Stoof, R. A. Duine, M. Polini, and G. Vignale, Phys. Rev. A **86**, 063631 (2012).
 - [57] T. Enss and R. Haussmann, Phys. Rev. Lett. **109**, 195303 (2012).
 - [58] G. Wlazłowski, P. Magierski, J. E. Drut, A. Bulgac, and K. J. Roche, Phys. Rev. Lett. **110**, 090401 (2013).
 - [59] H. Tajima, T. Kashimura, R. Hanai, R. Watanabe, and Y. Ohashi, Phys. Rev. A **89**, 033617 (2014).
 - [60] H. Tajima, R. Hanai, and Y. Ohashi, Phys. Rev. A **93**, 013610 (2016).
 - [61] H. Tajima, R. Hanai, and Y. Ohashi, Phys. Rev. A **96**, 033614 (2017).
 - [62] S. Jensen, C. N. Gilbreth, and Y. Alhassid, arXiv:1801.06163 [cond-mat.quant-gas].
 - [63] E. J. Mueller, Rep. Prog. Phys. **80**, 104401 (2017).
 - [64] S. Tsuchiya, R. Watanabe, and Y. Ohashi, Phys. Rev. A **80**, 033613 (2009).
 - [65] S. Tsuchiya, R. Watanabe, and Y. Ohashi, Phys. Rev. A **82**, 033629 (2010).
 - [66] S. Tsuchiya, R. Watanabe, and Y. Ohashi, Phys. Rev. A **84**, 043647 (2011).
 - [67] R. Watanabe, S. Tsuchiya, and Y. Ohashi, Phys. Rev. A **82**, 043630 (2010).
 - [68] E. J. Mueller, Phys. Rev. A **83**, 053623 (2011).
 - [69] P. Magierski, G. Wlazłowski, and A. Blugac, Phys. Rev. Lett. **107**, 145304 (2011).

- [70] S-Q. Su, D. E. Sheehy, J. Moreno, and M. Jarrell, Phys. Rev. A **81**, 051604(R) (2010).
- [71] J. T. Stewart, J. P. Gaebler, and D. S. Jin, Nature **454**, 744 (2008).
- [72] J. P. Gaebler, J. T. Stewart, T. E. Drake, D. S. Jin, A. Perali, P. Pieri, and G. C. Strinati, Nat. Phys. **6**, 569 (2010).
- [73] Y. Sagi, T. E. Drake, R. Paudel, R. Chapurin, and D. S. Jin, Phys. Rev. Lett. **114**, 075301 (2015).
- [74] A. Schnell, G. Röpke, and P. Schuck, Phys. Rev. Lett. **83**, 1926 (1999).
- [75] D. Lee and Thomas Schäfer, Phys. Rev. C **73**, 015202 (2006).
- [76] T. Abe and R. Seki, Phys. Rev. C **79**, 054002 (2009).
- [77] E. Timmermans, P. Tommasini, M. Hussein, and A. Kerman, Phys. Rep. **315**, 199 (1999).
- [78] M. Holland, S. J. J. M. F. Kokkelmans, M. L. Chiofalo, and R. Walser, Phys. Rev. Lett. **87**, 120406 (2001).
- [79] Y. Ohashi and A. Griffin, Phys. Rev. Lett. **89**, 130402 (2002).
- [80] X.-J. Liu and H. Hu, Phys. Rev. A **72**, 063613 (2005).
- [81] N. M. Hugenholtz and D. Pines, Phys. Rev. **116**, 489 (1959).
- [82] T.-L. Ho, X. Cui, and W. Li, Phys. Rev. Lett. **108**, 250401 (2012).
- [83] Y. Ohashi and A. Griffin, Phys. Rev. A **72**, 013601 (2005).
- [84] A. Perali, P. Pieri, G. C. Strinati, and C. Castellani, Phys. Rev. B **66**, 024510 (2002).
- [85] S. Tan, Ann. Phys. **323**, 2952 (2008).
- [86] S. Tan, Ann. Phys. **323**, 2971 (2008).
- [87] S. Tan, Ann. Phys. **323**, 2987 (2008).
- [88] K. Kamikado, T. Kanazawa, and S. Uchino, Phys. Rev. A **95**, 013612 (2017).
- [89] F. Palestini, A. Perali, P. Pieri, and G. C. Strinati, Phys. Rev. A **82**, 021605(R) (2010).
- [90] J. Carlson, S. Gandolfi, K. E. Schmidt, and S. Zhang, Phys. Rev. A **84**, 061602(R) (2011).
- [91] G. A. Baker, Jr., Phys. Rev. C **60**, 054311 (1999).
- [92] G. Zürn, T. Lompe, A. N. Wenz, S. Jochim, P. S. Julienne, and J. M. Hutson, Phys. Rev. Lett. **110**, 135301 (2013).
- [93] C. Sanner, E. J. Su, A. Keshet, W. Huang, J. Gillen, R. Gommers, and W. Ketterle, Phys. Rev. Lett. **106**, 010402 (2011).
- [94] A. Sommer, M. Ku, G. Roati, and M. W. Zwierlein, Nature **472**, 201 (2011).
- [95] J. Meineke, J.-P. Brantut, D. Stadler, T. Müller, H. Moritz, and T. Esslinger, Nat. Phys. **8**,

454 (2012).

- [96] S. Floerchinger, M. Scherer, S. Diehl, and C. Wetterich, Phys. Rev. B **78**, 174528 (2008).
- [97] Z.-Q Yu, K. Huang, and L. Yin, Phys. Rev. A **79**, 053636 (2009).
- [98] L. Pisani, A. Perali, P. Pieri, and G. C. Strinati, arXiv:1712.04666 [cond-mat.supr-con].
- [99] M. Ota, H. Tajima, R. Hanai, D. Inotani, and Y. Ohashi, Phys. Rev. A **95**, 053623 (2017).